Constraints on the G1/S transition pathway may favor selection of simple multicellularity as a passenger phenotype

Tom Louis Ducrocq, Damien Laporte and Bertrand Daignan-Fornier*

Univ. Bordeaux, CNRS, IBGC, UMR 5095, F-33000 Bordeaux, France

ORCID : TLD (0009-0009-6148-4057); DL (0000-0002-1556-5253); BDF (0000-0003-2352-9700)

*Corresponding author
bertrand.daignan-fornier@u-bordeaux.fr

ABSTRACT

Multicellularity is present throughout the entire tree of life. While the formation of simple multicellular entities can result from aggregation of cells or clonal development, it is not yet fully understood how, once formed, these simple multicellular entities could be maintained or even selected for. Here, using the yeast mutant *ace2* snowflake as a model of simple multicellularity, we aimed at identifying genetic conditions favoring its maintenance. Growth-competition experiments revealed that, while the *ace2* mutation by itself does not provide any advantage or disadvantage, the *ace2* snowflakes were strongly selected when combined to conditions affecting regulators of the G1/S transition of the cell cycle, such as Cln3 or Whi5. We show that this selection results from a faster exit from stationary phase of the *ace2* snowflake. Importantly, this advantage is not dependent on the multicellular phenotype, but rather on the *ace2* genotype itself. We found that the *ace2* selective advantage in the *cln3* background fully depends on the *KSS1* gene, another target of the Ace2 transcription factor. Finally, we show that results similar to those obtained with *ace2* mutants are phenocopied by the $AMN1^{368D}$ allelic form found in all feral yeast strains, hence bringing a strong physiological relevance to these observations. Altogether, our results support the hypothesis that simple multicellularity could persist, not because it provides a direct selective advantage due to multicellularity itself, but rather as a passenger phenotype that is maintained alongside other selected traits.

SIGNIFICANCE

While appearance of simple multicellularity does not seem so rare during evolution, what drove its maintenance and kept these simple multicellular entities away from counter-selection long enough for them to evolve sophisticated modes of cooperation such as division of labor, is questioning. A simple type of explanations is that multicellularity by itself could be advantageous, for example by allowing to escape predation or favoring resistance to stresses. Here we show that, alternatively, multicellularity can be selected as a phenotypic passenger of a mutation that is selected for another reason i.e. regulation of cell cycle progression. This initial absence of selective pressure on multicellularity itself may offer favorable conditions for further evolution.

INTRODUCTION

Multicellularity has evolved repeatedly and independently in distinct lineages within bacteria, archaea and eukaryotes (1). This evolutionary process firstly involves the selection of simple and initial forms of multicellularity like clusters of cells. Several selective drivers of simple multicellularity have been proposed (2) that are due to changes in geometry allowing access to new resources (faster sedimentation, increased mobility, foraging, dispersal), as well as other advantages associated with size increase (predation avoidance, stress resistance, improved extracellular metabolism) and finally, chimerism, the capacity to combine different cellular phenotypes in a single entity, allows the establishment of intra-organism division of labor.

Many forms of multicellularity are facultative and their formation is triggered by external signals. One of the best studied case is that of the slime mold *Dictyostelium discoideum*, which cells, in response to resource limitation, aggregate to form a fruiting body that favors dispersal of spores (3, 4). Another example comes from *Saccharomyces cerevisiae* yeast cells that, under poor nitrogen conditions, can become highly polarized and stay attached, thereby favoring foraging, a phenomenon known as pseudohyphal growth (5, 6). In such cases, multicellularity provides additional options to the non-proliferation observed in unicellular organisms in response to local nutritional starvation (7). These multicellularity-specific responses are triggered by nutritional cues and, plausibly, they may have evolved by functional recruitment of unicellular pre-existing sensors and pathways. It is hence rather likely that some actors of nutritional control of cell cycle progression should also be found as modulating facultative multicellularity. Indeed, there are several experimental evidences connecting the regulators of G1/S transition in the cell cycle to multicellularity. This mostly concerns two major regulators, retinoblastoma (RB) and Cyclin D. RB is a negative regulator of E2F, a transcription factor critical for G1/S progression, while cyclin D is a negative regulator of RB (8).

Notably, evidences connecting G1/S transition regulators to multicellularity come from studies on phylogenetically distant organisms. First, when the retinoblastoma (RB) cell cycle regulator from the simple multicellular volvocine *Gonium pectorale* was expressed in its close unicellular relative *Chlamydomonas*, the C*hlamydomonas* cells behaved as a simple multicellular colonial entity (9). This points to an important role for RB in triggering uni- to multicellular transition. Interestingly, in the aggregative multicellular slime mold, *Dictyostelium discoideum*, the RB orthologue, RblA, was found to be involved in the stalk *vs* spore cell-fate preference (10). Another key regulator of G1/S transition, namely Cyclin D, has also been associated to uni- to multicellular transition in two different yeast species, *Candida albicans* and *Saccharomyces cerevisiae*. Depending on environmental conditions, *Candida albicans* can grow in a yeast unicellular planktonic form, or in a filamentous multicellular

hyphal form. The transition from one form to the other is associated with invasion and virulence. Strikingly, the knock-down of the *C. albicans* cyclin D orthologue Cln3 resulted in hyphal growth suggesting that the G1 phase of the cell cycle is important in the transition from uni- to multicellular development in *C. albicans* (11). Similarly, in *S. cerevisiae* deletion of *CLN3*, the yeast cyclin D homolog, enhanced pseudohyphal growth (12). Interestingly, *CLN3* encodes an inhibitor of Whi5 which is the yeast functional equivalent of RB. It hence seems that, during evolution, uni- to multicellularity transitions have repeatedly used pre-existing regulators of the G1/S transition, such as RB and cyclin D. Although the pathways used might be the same, the precise outcome would be specific to each species in response to defined environmental conditions. Some of these intriguing results can be understood as the result of cooption processes where the pre-existing G1/S regulatory pathway was repeatedly and independently used by multicellularity to evolve. In other cases, the evolution of the G1/S regulation pathway itself could have somehow favored multicellularity emergence and/or maintenance.

In this work we used *S. cerevisiae* to further question this complex relationship between the cell cycle regulators and multicellularity. We took advantage of the snowflake model (13, 14) in which multicellularity is due to a genetic defect in cell separation. This form of multicellularity is dependent on specific mutations, most commonly a mutation of the Ace2 transcription factor (15, 16), and is therefore not dependent on external conditions. It follows that the uni- and multicellular yeast forms can be co-cultivated allowing to accurately compare their fitness. We observed that deletion of the *CLN3* gene, as well as the overexpression of the *WHI5* gene, favored the *ace2* snowflake form. We show that exit from stationary phase is the critical stage in which the *ace2 cln3* snowflakes are selected and that the *ace2* mutation, but not the snowflake phenotype, is responsible for the *cln3* faster quiescence exit phenotype. Finally, we establish that in haploid yeast, the natural (non-domesticated) $AMN1^{368D}$ allelic-form phenocopies both the multicellularity and the suppression phenotypes of the *ace2* mutant toward variations in the regulation of the G1/S transition. Our results point to the possibility that evolution of cell cycle control could promote the evolution of multicellularity, thus acting as a selective driver of simple multicellularity

RESULTS

The *ace2 cln3* snowflake strain is selected over the *ACE2 cln3* planktonic strain.

In order to investigate the relationship between the G1/S cell cycle regulators and multicellularity, we used the yeast snowflake model in which the absence of Ace2, a transcription activator of several chitinase and endoglucanases genes (17–19), results in the lack of separation of the daughter cell from

the mother cell. It ensues that *ace2* mutant yeasts form cell clusters that grow and end-up breaking most probably due to mechanical constraints (20). A major advantage of studying snowflakes rather than inducible forms of multicellularity, such as pseudo-hyphae, is that unicellular (planktonic, PK) and multicellular (snowflake, SF) yeast differing only by one mutation in the *ACE2* gene can be co-cultivated and their fitness can thus be assessed. We hence grew isogenic diploid *ACE2*/*ACE2* and *ace2*/*ace2* cells in minimal rich medium (SD casa WAU). Cultures of both genotypes were mixed to obtain a 50/50 mix of *ace2* SF and *ACE2* PK strains, either at the entity phenotype level (50/50 SF and PK ratio) or at the cell genotype level (50/50 *ace2* and *ACE2 ratio*) (Fig. 1A). The mixtures were then repeatedly grown to saturation and diluted every 2 days, resulting in a total of more than 100 generations. At each dilution point in each culture, the percentage of SF, defined as entities of at least 4 cells (Supplemental figure 1A), was estimated. Interestingly, in the BY (S288c-derived) background and in the SD casa WAU medium, the *ace2* SF strain showed no selective advantage or disadvantage over the *ACE2* PK strain, both at the SF phenotype level (Fig. 1B, black bars) and at the *ace2* genotype level (Fig. 1C, black bars). This indicates that the *ace2* mutation and its simple multicellular phenotype are not deleterious under the conditions used.

Strikingly, when similar experiments were performed with *ace2* or *ACE2* strains carrying a deletion of the *CLN3* gene, resulting in a longer G1 phase and larger cells (21), the *ace2* snowflake strains were rapidly enriched and took over the whole population (red bars, Fig. 1B-C). These results establish that *CLN3* and *cln3* cells behave quite differently in an *ace2* snowflake background. A similar result was obtained through overexpression of *WHI5* the major downstream target of *CLN3*. This was done by comparing the proportion of snowflake in a mixture of *ACE2* and *ace2* strains transformed either with an empty multicopy plasmid (black bars, Fig. 1D) or with a multicopy plasmid carrying the *WHI5* gene (red bars, Fig. 1D). This result showed that overexpression of *WHI5* phenocopied the *cln3* knock-out, indicating that the observed effect takes place through the well characterized G1/S transition regulatory pathway. Together our results reveal a robust phenotypic interaction between the G1/S transition major players, *CLN3* and *WHI5*, and the *ace2* snowflakes.

ace2 cln3 **exit faster from stationary phase than** ***ACE2 cln3***

In our competition experimental setup (Fig. 1A), the cultures alternate phases of exponential growth with phases of no growth, commonly referred as stationary phase (Supplemental figure 2A). Theoretically, the fitness advantage of the *ace2 cln3* strains over their *ACE2 cln3* isogenic counterparts could be due to a faster doubling time during exponential growth, to a higher biomass yield of the population, to a better survival in stationary phase or to a faster exit from stationary phase, each of

these factors (schematized in Supplemental figure 2A) acting either alone or combined. We thus tested these four possibilities separately. First, we found that the population doubling times of the two sets of strains was not significantly different (Supplemental figure 2B). In addition, *ace2* and *ACE2* cell populations led to similar biomass accumulation indicating that the yield of carbon utilization is not significantly modified by the *ace2* mutation (Supplemental figure 2C). We then estimated survival in the stationary state phase by staining cells grown for two days with methylene blue, a dye that specifically accumulates in dead cells. No significant differences in dead cell percentages were observed between *ace2* and *ACE2* cells should they be *cln3* or *CLN3* (Supplemental figure 2D). From these experiments, we conclude that neither lower doubling time, nor higher biomass yield, nor lower death rate could explain the selective advantage of the *ace2 cln3* cells over their *ACE2 cln3* counterpart.

We then compared the time required for populations of *ace2 cln3* and *ACE2 cln3* cells to exit stationary phase. Clearly, we found that the time required for proliferation to resume following refeeding, referred to as lag-time, was not significantly different between *ace2 CLN3* and *ACE2 CLN3* cells (grey and black dots, Fig.2A). We also observed that the lag-time was significantly longer for the *ACE2 cln3* (light red dots) than for *ACE2 CLN3* cell population (black dots) (Fig. 2A), as previously described (22, 23). Importantly, this difference was partially but significantly suppressed in *ace2 cln3* (red dots) cell population (Fig. 2A) suggesting that the *ace2* mutation genetically suppresses the *cln3* strain lag-time defect. The conclusion that *ace2 cln3* exit faster from stationary phase than *ACE2 cln3* obtained at the population level was confirmed at the individual cell level. This was done by refeeding quiescent cells from a stationary phase culture on agarose pads under the microscope as illustrated in Fig. 2B (*ace2 cln3*; *ACE2 cln3*), and by monitoring the proportion of cells that formed a new bud upon refeeding, corresponding to the cells that have entered a new cell cycle. The proportion of cells that formed a bud upon refeeding was not significantly different between *ace2 CLN3* and *ACE2 CLN3* strains (Supplemental figure 2E). By contrast it was significantly higher for the *ace2 cln3* cells than for the *ACE2 cln3* cells all along the experiment on agarose pad (Fig. 2C). This result strongly reinforced our conclusions obtained from cell populations (Fig. 2A). Importantly, a similar set of observations was made with haploid *ace2 cln3* cells (Fig. 2D) where snowflakes are much smaller (Supplemental figure 2G-K) due to smaller cell size but also to the proximal budding pattern of haploid cells that make snowflakes much more globular, while diploid *ace2* mutants form more elongated and radial clusters (24). This observation confirmed the robustness of the observed initial *cln3* phenotype and its suppression by *ace2*. Altogether these results point to stationary phase exit as the key step accounting for the competition outcomes.

A simple prediction from these results is that a competition experiment ran under conditions where the cells are always maintained in exponential growth should not result in any fitness advantage for

ace2 cln3 strains over *ACE2 cln3*. Indeed, co-culturing these two strains in exponential phase for 94hrs (corresponding to at least 70 generations), did not result in any fitness advantage for the snowflake population (Fig. 2E, left panel), by contrast to an equivalent number of generations encompassing cycles of proliferation and stationary phases (Fig. 2E, right panel). Conversely, increasing the duration of stationary phase resulted in a longer exit time (Fig. 2F), as described previously (25). Importantly, it also increased the fitness advantage of *ace2 cln3* over *ACE2 cln3* cells (red and pink bars Fig. 2G), while there was still no difference between *ace2 CLN3* and *ACE2 CLN3* cells (black and grey bars Fig. 2G). Altogether, our results pinpoint exit from stationary phase as the critical stage in which the *ace2 cln3* snowflakes are positively selected.

The advantage of *ace2 cln3* during quiescence exit is independent of the snowflake phenotype

Why would *ace2 cln3* cells exit quiescence faster than *ACE2 cln3* cells? This could be due to a specificity associated with *cln3* mutation that would modify the snowflake properties. Alternatively, it could be dependent on the specific *ace2 cln3* mutation combination independently of the snowflake phenotype. To answer this question, we dissociated the SF phenotype from the *ace2* mutation and vice versa.

First, we asked whether the snowflake phenotype is sufficient, independently of the *ace2* mutation, to make quiescent exit faster when combined with *cln3*. Ace2 is a transcription factor that allows expression of several chitinases and endoglucanases necessary for septal digestion and cell separation at cytokinesis. To mimic the *ace2* snowflake phenotype, we constructed a quintuple chitinase and endoglucanase mutant (*cts1, dse2 dse4, egt2, scw11*), hereafter "quintuple mutant", that results in a snowflake phenotype comparable to that of the *ace2* mutant (Fig. 3 A-C) while carrying the wild-type *ACE2* allelic form. This quintuple mutant, when combined with the *cln3* mutation, had no effect on the timing of quiescence exit (Fig. 3D) suggesting that it is the *ace2* mutation itself that suppresses the slower exit defect of the *cln3* mutant. This was confirmed by comparing quiescence exit after refeeding of a *cln3* quintuple mutant with a *cln3 ace2* mutant. While both strains were predominantly comprising snowflakes, the kinetic of exit from quiescence after refeeding was much faster for the *cln3 ace2* strain (Fig. 3E). Finally, competition experiments confirmed that the snowflake phenotype is not sufficient to give the *cln3* mutant a phenotypical advantage (Fig. 3F).

We then asked whether the *ace2* mutation itself, independently of the snowflake phenotype, could be sufficient to make quiescent exit faster when combined with *cln3*. We thus examined whether planktonic cells obtained in an *ace2* mutant background would still behave as their snowflake counterparts. This was done by sonicating *ace2 cln3* before refeeding and exit from quiescence. While,

mild sonication resulted in an increase of planktonic cells in the population (up to 50% with no effect on lethality, supplementary figure 4A-B), neither isolated cells, nor small or large cell clusters after sonication had a significantly different quiescence exit speed measured by budding index (Fig. 4A). Accordingly, *cln3 ace2* isolated cells resulting from sonication still exited quiescence faster than their *cln3 ACE2* sonicated counterpart (Fig. 4B). The sonicated and non-sonicated cells had the same exit kinetics, indicating that sonication *per se* had no significant impact on quiescence exit (supplementary figure 4C). These results show that the snowflake phenotype is not necessary for the *ace2 cln3* mutant to exit quiescence faster than *ACE2 cln3*. Altogether our data establish that the *ace2* mutation, but not the snowflake phenotype, is responsible for the *cln3* faster quiescence exit phenotype.

The faster *ace2 cln3* quiescence exit is dependent on the Kss1 MAP kinase

Why is the *cln3* mutant slower at exiting quiescence and why is this phenotype suppressed by the *ace2* deletion? Upon refeeding of stationary cultures, *CLN3* transcription is increased 5- to 10-fold within 5 min (23). Cln3 is hence likely to play an important role for quiescent cells to move out from G1 and reenter proliferation. Accordingly, a delay of *cln3* mutants to exit quiescence was previously documented (23). The question here is then: how does the *ace2* mutation suppress this growth delay? Among the well-established targets of Ace2, as a transcription factor, are *AMN1*, *BUD9, CHS7, CTS1, DSE2, DSE4, KSS1* and *SCW11* (17). Four of those, namely *CTS1, DSE2, DSE4* and *SCW11*, are not involved in suppressing the delay phenotype since they are mutated in the quintuple mutant that, in combination with *cln3*, has the same delay as a single *cln3* mutant (Fig. 3D). We focused on Kss1, a MAP kinase involved in filamentous growth and mating (26, 27), because the Kss1 pathway was previously found to positively regulate another G1 cyclin gene, *CLN1* that is partially redundant to *CLN3* (28). Deletion of the *ACE2* gene results in higher *KSS1* expression (17) that could lead to higher *CLN1* expression and thereby be responsible for the *cln3* mutation suppression. We hence tested whether suppression of *cln3* by *ace2* was dependent on *KSS1* by comparing quiescence exit of *ace2 cln3 KSS1* and *ace2 cln3 kss1* cells. Clearly, the deletion of *KSS1* totally abolished the suppression of *cln3* by *ace2* (Fig. 5A). Accordingly, *CLN1* expression during stationary phase exit was significantly higher in the *ace2 cln3* than in the *ACE2 cln3* strain (Fig. 5B) and this differential expression was fully abolished in the absence of *KSS1* (Fig. 5C). We conclude that the competitive advantage of the *ace2* mutant over its *ACE2* wild-type counterpart is most likely due to higher expression of *CLN1* that, at least partially, compensates for the absence of *CLN3*. Importantly, this transcriptional effect of Ace2 on *CLN1*, via Kss1, is independent of the role of Ace2 on multicellularity.

The *AMN1^{368D}* allelic-form, found in budding yeast in the wild, phenocopies the *ace2* deletion

In laboratory strains, the Ace2 protein level is constant throughout the cell cycle, while in feral strains this is clearly not the case (24). This is due to the presence of the recessive *amn1^{368V}* allelic form in laboratory strains, which was probably initially selected to avoid "unwanted" cell clusters in lab yeast strains. The "natural" *AMN1^{368D}* allelic-form results in proteolysis of Ace2 through the ubiquitin proteasome system (24). This protein degradation mostly takes place in haploid cells, which are snowflake, while diploids are planktonic (24). It thus appears that the Amn1/Ace2 tandem has an important physiological role associated with optional post-mitotic cell separation in a ploidy-dependent fashion. We first showed that *AMN1^{368D}* results in a snowflake phenotype comparable to that of *ace2* mutant strains (Fig. 6A-C). We then asked whether *AMN1^{368D}* could suppress the quiescence exit delay of the *cln3* mutant. Indeed, the *cln3 AMN1^{368D}* strain exited quiescence much more rapidly than the *cln3 AMN1^{368V}* strain (Fig. 6D). Finally, we found that *AMN1^{368D}* was strongly enriched in competition experiments when associated with a *cln3* mutation (Fig. 6E) or overexpression of *WHI5* (Fig. 6F). We conclude that, in haploid yeast, the natural (non-domesticated) *AMN1^{368D}* allelic-form phenocopies both the multicellularity and the suppression phenotypes of the *ace2* mutant toward variations in the regulation of the G1/S transition.

DISCUSSION

In this work, we reveal a genetic connection between major actors of G1/S progression in the cell cycle and the *AMN1* and *ACE2*, key actors modulating cell cohesion at the end of mitosis (Fig. 7). Interestingly, this connection operates differently in laboratory strains (Fig. 7A) and feral strains (Fig. 7B) due to a polymorphism at the *AMN1* locus, most probably selected upon lab strains implantation. We established that, in our experimental setup, this genetic interaction is due to the pleiotropy of the *ace2* mutation, affecting not only the chitinases and endoglucanases that are critical for septum digestion and cell separation, but also the Kss1 MAP kinase which contributes to the activation of Cln1, one of the G1 cyclins. From this pleiotropic effect of the *ace2* mutation we draw two inferences, one practical is that the phenotypes associated with the *ace2* mutation, which is often used to generate snowflake multicellularity in yeast, should be considered cautiously and not necessarily attributed to multicellularity. The second inference is that in some instances, multicellularity may have evolved as a passenger phenotype of another phenotype that was the one selected (Fig. 7B). We propose that such a selective mechanism could contribute to favor the exaptation of more complex traits associated with multicellularity.

Because the snowflake model of multicellularity is genetically determined, by *ace2* or *AMN1*^{368D} and not triggered by external cues, as it is often the case for facultative multicellularity, our experimental design allows direct fitness measurements between uni- and multicellular entities. Interestingly, in a wild-type background, multicellularity was not counter-selected, even following a substantial period of co-culture. Such a neutral effect of multicellularity on fitness could easily result in phenotypical *aller-retours* between unicellularity and multicellularity during evolution. In *S. cerevisiae*, the *AMN1*^{368D} allele found in wild yeast is placed under control of the Ste12 transcription factor that is only active in haploid cells (24). It follows that diploid strains are planktonic while haploid strains form clusters (29). How this complex pattern was initially selected remains to be established, but our results indicate that it could have been biased by the evolution of the cell cycle regulation.

Previous work on *Gonium pectorale*, a simple multicellular form of volvocine green algae, has established that expression of the *Gonium* Rb homolog in the unicellular volvocine *Chlamydomonas reinhardtii* was sufficient to induce a colonial form of multicellularity. The authors conclude that the mechanism of multicellular evolution is primarily cooption and regulatory modification of existing pathways such as cell cycle progression and its complex regulation. Here we show that the *ace2* or *AMN1*^{368D} mutations are sufficient to counteract a phenotypic effect of the overexpression of the Rb functional orthologue Whi5 (Fig. 1D, Fig. 6F). Our results hence suggest that the co-evolution of cell cycle regulation and multicellularity could be a much more general feature than first thought. It could have started very early in the evolution of eukaryotic cells or alternatively could be a case of convergent evolution. Importantly regulator genes of the G1/S transition are among the most frequent drivers of cancer, the RB gene being generally mutated while cyclin D being overexpressed through various means (30, 31). Because the link between cancer and multicellularity is regularly questioned (32, 33), understanding the role of these G1/S regulators in multicellularity in parallel to their role in cancer is particularly relevant.

More generally, our results prompt us to reconsider whether simple multicellularity, which appeared multiple times in evolution, was always selected for the new physical and physiological properties it provides (2). Alternatively, it is possible that multicellularity was initially selected as a byproduct, allowing it to be maintained although not necessarily increasing fitness as such. This would contribute to disconnect the initial selection of simple multicellularity from the selection of further associated advantages, such as division of labor, that would require time and necessitate that the multicellularity phenotype would not be counter-selected in the first place. Such a passenger selection of multicellularity would make it independent of physical constraints such as size or shape that could bias its further evolution. The work presented here provides a proof of concept that such a scenario is plausible and may have contributed to the multiple appearance of multicellularity in the tree of life.

MATERIALS AND METHODS

Yeast media and strains, plasmids and oligonucleotides

Yeast cells were grown in liquid or solid media at 30 °C. SD is a synthetic minimal medium containing 0.5% ammonium sulfate, 0.67% yeast nitrogen base (Difco), 2% glucose. SDcasaWAU is an SD medium supplemented with 0.2% casamino acids (Difco) tryptophan (0.2 mM), adenine (0.3 mM) and uracil (0.3 mM). Unless specified, cells were grown in SDCasaWAU medium. When indicated, medium was depleted in uracil, resulting in a medium named SDCasaWA, allowing the selection of cells expressing a vector carrying *URA3* marker. SC medium was prepared as described by Sherman (34) and was supplemented by histidine (0.06 mM), leucine (0.5 mM), lysine (0.07 mM), tryptophan (0.2 mM), adenine (0.3 mM), and uracil (0.3 mM). The medium obtained by the depletion of both uracil and leucine, called SC-U-L medium, allows the selection of cells expressing both *URA3* and *LEU2* markers. The YPD medium contained 1% yeast extract, 2% peptone, and 2% glucose.

Yeast strains (listed in Table 1) are derived from both FY4 and FY5 prototrophic strains and from disrupted strains isogenic to BY4741 or BY4742 purchased from Euroscarf (Frankfurt, Germany). Strains described in Table 1 were either obtained by crossing, sporulation, and micromanipulation of meiosis progeny or by transformation of cells with a DNA fragment of interest (plasmid, PCR product). Yeast strains were transformed using the lithium acetate method (35).

All plasmids and oligonucleotides are listed in Tables 2 and 3, respectively. To construct the plasmids allowing the overexpression of *WHI5* in yeast strains, the open reading frame of the *WHI5* gene was amplified using the genomic DNA of the FY4 strain as a template. The PCR product was then cloned into two 2µ vectors, YEpLac195 and YEpLac181, carrying respectively *URA3* and *LEU2* markers. Two plasmids carrying respectively two different alleles of *AMN1* gene were also constructed. The open reading frame of the *AMN1* gene was amplified using either the FY4 strain genomic DNA (*AMN1-368V* PCR product) or the GN-1C strain genomic DNA (*AMN1-368D* PCR product). The GN-1C strain was a generous gift from Pr. Marullo. The PCR products were cloned into YIpLac211, that allowed integration of the cloned *AMN1* allele at the yeast *AMN1* locus.

Description of a Snowflake population

Snowflake population or co-culture between Snowflake and Planktonic strains were observed in a Kova Glasstic slide (Kova international, 87144F). The proportion of the Snowflake phenotype in these

populations was determined by counting entities formed by four or more cells. To characterize the size of Snowflakes within a population, the population was observed between slide and coverslip separated by a layer of double-sided adhesive tape. The longest segment of the Snowflake entity was measured, as well as the longest segment perpendicular to the first segment and lying in the same Z plane.

Competitions experiment in co-culture

Snowflakes strains (either *ace2* or quintuple mutant or *AMN1-368D*) and planktonic strains were grown in monocultures to stationary phase, for 2 days unless specified. Snowflake and planktonic strains were then mixed in indicated proportion and co-cultured. Unless specified, every 2 days, co-cultures were diluted after they reached stationary phase by a factor of 1000 into fresh liquid medium.

To set up co-cultures for which the proportion of Snowflake phenotype was monitored throughout the competition, the entity (Snowflake entity or single-cell entity) concentrations in each of the monocultures were determined. The volumes of the 2 monocultures in the mix were accordingly determined and then adjusted to obtain 50% of Snowflake entity in the mix. The proportion of Snowflakes in the co-culture was determined every two days before dilution in fresh medium.

To set up co-cultures for which the proportion of *ace2* genotype was monitored throughout the competition, the two strains were mixed to obtain a 50/50 ratio. Every 2 days, the genomic DNA of the stationary phase co-cultures was extracted by phenol-chloroform protocol. Quantitative PCR amplifications were then performed with GoTaq® qPCR Master Mix (Promega, A6001), using 50ng of DNA extracted from co-cultures. The first set of primers was designed to amplify the *ace2::KanMX4* locus with the first primer targeting the region directly upstream of the ATG of the *ACE2* gene, and the second primer targeting a region specific to the *KanMX4* marker (Table3). The second set of primers targeted a region of *ACT1* gene (Table3).

For competitions in which the co-cultures were maintained in proliferation phase for 94 hours, the co-cultures were diluted every 8 hours to ensure that the OD_{600nm} was always maintained below 0.5.

Population measurement

To determine the population doubling time of yeast strains, cells were kept in exponential proliferation phase ($OD_{600nm} \leq 1.0$) for at least 24 hours by successive dilutions before any measurement. Population doubling time was then determined by following cell number during 5 hours on at least three independent exponential growth culture measuring the optical density at 600 nm. Population doubling

time was then determined by exponential growth regression of the proliferation curves using GraphPad Prism 8 (GraphPad Software, Inc. La Jolla, USA).

Cells were stained with a solution containing 0.2% of methylene blue (Sigma-Aldrich, Saint Louis, MI, USA) and 2% sodium citrate pH7 to determine the cell viability. After 5 minutes of incubation, the proportion of blue-stained dead cells was scored.

The biomass yield of cultures was determined by filtration of 2 days stationary phase cell cultures on 0.45 µm polyamide pre-weighted filters (25006–47-N; Sartorius). The filter was washed twice with 10 mL of miliQ water and then dried with successive 30 seconds cycles in a microwave oven at 800 W until the mass of the filter and cells was constant. The filtered volume of culture was adjusted to correspond to at least 10 mg of dry biomass.

Refeeding of stationary phase cultures

Unless the age of cultures is otherwise specified, 2 day stationary phase liquid monocultures were refed either on liquid or solid fresh SDcasaWAU medium.

Stationary phase cultures were refed by dilution into liquid fresh SDcasaWAU medium at approximately 0.05 OD_{600nm}. The OD_{600nm} was monitored upon refeeding for at least 7 hours covering both 'lag' and exponential phases (until at least a 5-fold increase of the OD_{600nm} compared to the initial point). To quantify the duration of the 'lag' phase, we normalized all the OD_{600nm} values of each individual growth curve to their respective initial OD_{600nm} value and then applied the logarithmic function to all the normalized OD_{600nm} values of the growth curve. We next performed a linear regression on the points corresponding to the proliferation phase of the growth curve using GraphPad Prism 8 (GraphPad Software, Inc. La Jolla, USA). The time value for which the linear regression intersects the Time-X axis corresponds to the end of the 'lag' phase and the beginning of the proliferation phase, and is referred as 'the duration of lag phase'.

Stationary phase cultures were also refed onto solid medium. Cells were spread onto half a 3% agarose microscope pad made of fresh SDcasaWAU. Bright field images of individual cells were then captured every 15 minutes for up to 4 hours. The cells forming an unequivocal new bud upon refeeding were scored.

When indicated, an aliquot of stationary phase culture can be sonicated before a refeeding experiment on microscope agarose pad. Cycles of 30 seconds in a sonication bath were carried out until the

proportion of single-cell entities in the *ace2* SF culture increased to a desired proportion (approximately 40%).

Determination of CLN1 mRNA level upon refeeding by Reverse transcriptase-PCR.

To determine the level of *CLN1* mRNA upon refeeding of 2-day stationary phase cultures, 15 mL of a 2-day culture was diluted in 85 mL of fresh medium. Fifteen minutes upon refeeding, 25 mL of culture was sampled and centrifuged at 4000 rpm at 4°C for 3 min. The pellet was washed in 1 mL of RNase-free H2O, and centrifuged at 12,000 g at 4°C for 30 seconds. A Tri-Reagent (Sigma, T9424) protocol was then performed to extract total RNA. A reverse-transcription of 200ng of total RNA using the 'High Capacity cDNA Reverse Transcription' Kit (ThermoFisher, 4368813) was then performed. The cDNA was diluted to 1/25 and amplified with a Quantitative-PCR protocol, using the GoTaq® qPCR Master Mix (Promega, A6001) and primers specific to the coding region of *CLN1* or the coding region of *ACT1* (Table 3).

Microscopy

The refeeding experiments on microscope pad, as well as the Snowflake size-measurement experiments were carried out using a Zeiss 200M inverted microscope (Carl Zeiss, Thornwood, NY, USA) with the additional equipment : a MS-2000 stage (Applied Scientific Instrumentation, Eugene, OR, USA), a Lambda LS 300 W xenon light source (Sutter, Novato, CA, USA), a 5 positions filter turret, a 100X 1.4NA Plan-Apochromat objective and a CoolSnap HQ camera (Roper Scientific, Tucson, AZ, USA). The filters are from Chroma Technology Corp. The microscope and additional equipment were controlled by SlideBook software 5.0. (Intelligent Imaging Innovations, Denver, CO, USA). The images were analyzed with Image J. All other microscopy experiments were carried out using Zeiss Primo Star microscope, equipped with a 40X/0.65 Plan-Achromat objective.

Statistical analysis

All experiments were carried out at least three times on independent biological samples. The exact number of independent samples is indicated in figure legends. Data are presented as mean ± SD. All the statistical analyses were done using GraphPad Prism 8 (GraphPad Software, Inc. La Jolla, USA). The proportion of SF in competition experiments, the refeeding experiments on microscope pad and the proportion of dead cells were analysed by Fisher's exact test on a contingency table. Other

experiments are analyzed by Welch's unpaired t-test. p-values below 0.05 are represented by *; p values inferior to 0.005 are represented by **; and p values inferior to 0.001 are represented by ***. p-values superior to 0.05 were considered non-significant and are represented by 'ns'.

Table 1: Strains

Strain name	Genotype
FY4	
Y12580, Y12581, Y12582	*cln3::URA3/cln3::URA3 ura3Δ0/ura3Δ0 leu2Δ0/leu2Δ0*
Y12584, Y12585, Y12586	*ace2::KanMX4/ace2::KanMX4 cln3::URA3/cln3::URA3 ura3Δ0/ura3Δ0 leu2Δ0/leu2Δ0*
Y12606, Y12607, Y12608	*leu2Δ0/leu2Δ0*
Y12973, Y12974, Y12975	*ace2::KanMX4/ace2::KanMX4 leu2Δ0/leu2Δ0*
Y12575 + p5314	*ace2::KanMX4/ace2::KanMX4 ura3Δ0/ura3Δ0* carrying empty plasmid 2µ
(Y11418xY12599) + p5314	*ura3Δ0/ura3Δ0* carrying empty plasmid 2µ
Y12575 + p4726	*ace2::KanMX4/ace2::KanMX4 ura3Δ0/ura3Δ0* carrying plasmid 2µ *WHI5*
(Y11418xY12599) + p4726	*ura3Δ0/ura3Δ0* carrying plasmid 2µ *WHI5*
Y12512	*ace2::KanMX4/ace2::KanMX4 HTB1-3xCFP-LEU2/HTB1-3xCFP-LEU2 ura3Δ0/ura3Δ0 his3Δ1/HIS3*
Y12565, Y12566, Y12958	*ace2::KanMX4 cln3::URA3 ura3Δ0 leu2Δ0*
Y12567, Y12568, Y12959	*cln3::URA3 ura3Δ0 leu2Δ0*
Y12408, Y12595, Y12596	*ace2::KanMX4 leu2Δ0*
Y11417, Y12571	*leu2Δ0*
Y12709, Y12710, Y12711	*cln3::URA3/cln3::URA3 ura3Δ0/ura3Δ0 leu2Δ0/leu2Δ0*
Y12716, Y12717, Y12718	*dse2::KanMX4/dse2::KanMX4 cts1::KanMX4/cts1::KanMX4 scw11::KanMX4/scw11::KanMX4 egt2::KanMX4/egt2::KanMX4 dse4::KanMX4/dse4::KanMX4 cln3::URA3/cln3::URA3 ura3Δ0/ura3Δ0 leu2Δ0/leu2Δ0*
Y12976, Y12977, Y12978	*dse2::KanMX4/dse2::KanMX4 cts1::KanMX4/cts1::KanMX4 scw11::KanMX4/scw11::KanMX4 egt2::KanMX4/egt2::KanMX4 dse4::KanMX4/dse4::KanMX4 leu2Δ0/leu2Δ0*
Y12967, Y12968	*kss1::KanMX4 ace2::KanMX4 cln3::URA3 ura3Δ0 leu2Δ0*

Y12969, Y12970	*kss1::KanMX4 cln3::URA3 ura3Δ0 leu2Δ0*
Y12971	*CLN1-15Myc-HIS3 ura3Δ0 leu2Δ0 his3Δ1 lys2Δ0*
Y12838, Y12839, Y12840	*AMN1368D-URA3-AMN1368V ura3Δ0 leu2Δ0*
Y12935, Y12936, Y12937	*AMN1368V-URA3-AMN1368V ura3Δ0 leu2Δ0*
Y12942, Y12943, Y12944	*AMN1368D-URA3-AMN1368V cln3::KanR ura3Δ0 leu2Δ0 his3Δ1*
Y12946, Y12947, Y12949	*AMN1368V-URA3-AMN1368V cln3::KanR ura3Δ0 leu2Δ0 his3Δ1*
Y12838 + p338	*AMN1368D-URA3-AMN1368V ura3Δ0 leu2Δ0* carrying empty plasmid 2µ
Y12935 + p6053	*AMN1368D-URA3-AMN1368V ura3Δ0 leu2Δ0* carrying plasmid 2µ *WHI5*
Y12838 + p338	*AMN1368D-URA3-AMN1368V ura3Δ0 leu2Δ0* carrying empty plasmid 2µ
Y12935 + p6053	*AMN1368D-URA3-AMN1368V ura3Δ0 leu2Δ0* carrying plasmid 2µ *WHI5*
GN-1C	*HO:NatR AMN1368D FLO8+*

Table 2: Plasmids

Plasmid Name	Description	
p5314	YEpLac195: 2µ URA3 AmpR	Gietz *et al.* 1988
p4726	*WHI5* in YEpLac195	lab collection
p338	YEpLac181 : 2µ LEU2 AmpR	Gientz *et al*. 1988
p6053	*WHI5* in YEpLac181	This study
p6164	YIpLac211 : integrative plasmid URA3 AmpR	Gietz 1988
p6165	*AMN1-368D* in YIpLac211	This study
p6167	*AMN1-368V* in YIpLac211	This study

Table 3: Oligonucleotides

Oligonucleotide name	Sequence 5'-3'
qPCR locus ACE2 -26 forward	GGACCAAAAACGGTGTTAATACAATC
qPCR KanMX4 specific reverse	CTGGCGCGCCTTAATTAACC
qPCR ACT1 forward (coding)	CCCCAGAAGAACACCCTGTTC

qPCR ACT1 reverse (coding)	CGTAGAAGGCTGGAACGTTG
qPCR CLN1 coding forward	ATCGATCAGCAACCGGAGAT
qPCR CLN1 coding reverse	AACCTGACAGCGTGGAAGAA
KanB reverse	CTGCAGCGAGGAGCCGTAAT
ACE2 promoter forward	CGTCACTCCATTAGAATCCC
CLN3 promoter forward	TCCTCATTCGGTTTAACTCC
CLN3 terminator reverse	TGACTAGAGGAAGTAAGGAG
DSE2 promoter forward	CAGTAGAGCTAACCACAGTC
CTS1 promoter forward	ACTGTCGCTCGTTTCACAAC
SCW11 promoter forward	CAGTTACGCAACAAAGACAG
DSE4 promoter forward	ACTACAAGCGAGGGTAAAGG
EGT2 promoter forward	GATGCTGGTTTGATGCTAAG
CLN3 promoter -500 forward	TGAGGAAAGAGGACTATACC
CLN3 terminator +500 reverse	TAGGTAGCGATGAAGATTGG
URA3 promoter -500 forward	TCATCATCTCATGGATCTGC
URA3 terminator +500 reverse	TACGCCAGTACACCTTATCG
CLN1 promoter -200 forward	CCAAGGAGTTCTTCGTTCGC
CLN1 terminator +200 reverse	TCGCGTCATCTTTTCCGTTC
AMN1 promoter -75 forward	GTTTAATATCCATCCATTCC
AMN1 +459 forward	CCTTTGACTGCTCAACATCAG
AMN1 +882 forward	CATCAAGTAACACAACCAG
AMN1 +1269 forward	GGTTGTGATGTTGATGATG
AMN1 terminator +169 reverse	GTTTCTTCGGCCCTTCTGGA
AMN1 +1269 reverse	CATCATCAACATCACAACC
AMN1 +882 reverse	CTGGTTGTGTTACTTGATG
AMN1 +376 reverse	GAAAGACTGGATGCAGAAAC
Mat a and alpha forward	AGTCACATCAAGATCGTTTATGG
Mat a specific reverse	CTCCACTTCAAGTAAGAGTTTG
Mat alpha specific reverse	GCACGGAATATGGGACTACTTCG

WHI5 BamHI forward	CGCGGATCCCAAATCGGATATGAGCAGCTG
WHI5 PstI reverse	ACGTCTGCAGGCTCGAGGCGATCTGTCGC
M13 reverse	CAGGAAACAGCTATGACC
AMN1 BamHI forward	GTTGGATCCATGAAACTAGAACGCG
AMN1 PstI reverse	AACCTGCAGCTAGTCCACATTATTCTCTATTTCG

ACKNOWLEDGMENTS AND FUNDING SOURCES

The authors thank Benoît Pinson and Isabelle Sagot for discussions on the project. The authors also thank Sabine Vaur for her help with the qPCR method. This work was supported by a grant from Ligue Régionale Contre le Cancer (2022 Dordogne) to BD-F. TD was supported by a grant from University of Bordeaux, NewMoon RRI Program on Cancer in Evolution.

REFERENCES

1. R. K. Grosberg, R. R. Strathmann, The Evolution of Multicellularity: A Minor Major Transition? *Annu. Rev. Ecol. Evol. Syst.* **38**, 621–654 (2007).

2. K. Tong, G. O. Bozdag, W. C. Ratcliff, Selective drivers of simple multicellularity. *Current Opinion in Microbiology* **67**, 102141 (2022).

3. M. La Fortezza, K. Schaal, G. J. Velicer, Why Aggregate? On the Evolution of Aggregative Multicellularity. [Preprint] (2021). Available at: https://www.preprints.org/manuscript/202105.0451/v1 [Accessed 28 April 2025].

4. P. C. Newell, A. Telser, M. Sussman, Alternative Developmental Pathways Determined by Environmental Conditions in the Cellular Slime Mold *Dictyostelium discoideum*. *J Bacteriol* **100**, 763–768 (1969).

5. C. J. Gimeno, P. O. Ljungdahl, C. A. Styles, G. R. Fink, Unipolar cell divisions in the yeast S. cerevisiae lead to filamentous growth: Regulation by starvation and RAS. *Cell* **68**, 1077–1090 (1992).

6. A. Kumar, The Complex Genetic Basis and Multilayered Regulatory Control of Yeast Pseudohyphal Growth. *Annu. Rev. Genet.* **55**, 1–21 (2021).

7. B. Daignan-Fornier, D. Laporte, I. Sagot, Quiescence Through the Prism of Evolution. *Front. Cell Dev. Biol.* **9**, 745069 (2021).

8. C. Bertoli, J. M. Skotheim, R. A. M. De Bruin, Control of cell cycle transcription during G1 and S phases. *Nat Rev Mol Cell Biol* **14**, 518–528 (2013).

9. E. R. Hanschen, *et al.*, The Gonium pectorale genome demonstrates co-option of cell cycle regulation during the evolution of multicellularity. *Nat Commun* **7**, 11370 (2016).

10. H. MacWilliams, *et al.*, A retinoblastoma ortholog controls stalk/spore preference in *Dictyostelium*. *Development* **133**, 1287–1297 (2006).

11. C. Bachewich, M. Whiteway, Cyclin Cln3p Links G_1 Progression to Hyphal and Pseudohyphal Development in *Candida albicans*. *Eukaryot Cell* **4**, 95–102 (2005).

12. J. D. J. Loeb, T. A. Kerentseva, T. Pan, M. Sepulveda-Becerra, H. Liu, Saccharomyces cerevisiae G1 Cyclins Are Differentially Involved in Invasive and Pseudohyphal Growth Independent of the Filamentation Mitogen-Activated Protein Kinase Pathway. *Genetics* **153**, 1535–1546 (1999).

13. W. C. Ratcliff, J. T. Pentz, M. Travisano, TEMPO AND MODE OF MULTICELLULAR ADAPTATION IN EXPERIMENTALLY EVOLVED *SACCHAROMYCES CEREVISIAE*. *Evolution* **67**, 1573–1581 (2013).

14. W. C. Ratcliff, R. F. Denison, M. Borrello, M. Travisano, Experimental evolution of multicellularity. *Proc Natl Acad Sci U S A* **109**, 1595–1600 (2012).

15. W. C. Ratcliff, J. D. Fankhauser, D. W. Rogers, D. Greig, M. Travisano, Origins of multicellular evolvability in snowflake yeast. *Nat Commun* **6**, 6102 (2015).

16. J. H. Koschwanez, K. R. Foster, A. W. Murray, Improved use of a public good selects for the evolution of undifferentiated multicellularity. *eLife* **2**, e00367 (2013).

17. Y. Mostovoy, A. Thiemicke, T. Y. Hsu, R. B. Brem, The Role of Transcription Factors at Antisense-Expressing Gene Pairs in Yeast. *Genome Biol Evol* **8**, 1748–1761 (2016).

18. W. P. Voth, A. E. Olsen, M. Sbia, K. H. Freedman, D. J. Stillman, *ACE2* , *CBK1* , and *BUD4* in Budding and Cell Separation. *Eukaryot Cell* **4**, 1018–1028 (2005).

19. M. Doolin, A. L. Johnson, L. H. Johnston, G. Butler, Overlapping and distinct roles of the duplicated yeast transcription factors Ace2p and Swi5p. *Molecular Microbiology* **40**, 422–432 (2001).

20. S. Jacobeen, *et al.*, Cellular packing, mechanical stress and the evolution of multicellularity. *Nature Phys* **14**, 286–290 (2018).

21. R. Nash, G. Tokiwa, S. Anand, K. Erickson, A. B. Futcher, The WHI1+ gene of Saccharomyces cerevisiae tethers cell division to cell size and is a cyclin homolog. *The EMBO Journal* **7**, 4335–4346 (1988).

22. L. L. Newcomb, J. A. Diderich, M. G. Slattery, W. Heideman, Glucose Regulation of *Saccharomyces cerevisiae* Cell Cycle Genes. *Eukaryot Cell* **2**, 143–149 (2003).

23. M. Wu, L. Newcomb, W. Heideman, Regulation of Gene Expression by Glucose inSaccharomyces cerevisiae: a Role for ADA2and ADA3/NGG1. *J. Bacteriol.* **181**, 4755–4760 (1999).

24. O. Fang, *et al.*, Amn1 governs post-mitotic cell separation in Saccharomyces cerevisiae. *PLoS Genet* **14**, e1007691 (2018).

25. D. Laporte, L. Jimenez, L. Gouleme, I. Sagot, Yeast quiescence exit swiftness is influenced by cell volume and chronological age. *Microb Cell* **5**, 104–111 (2018).

26. W. E. Courchesne, R. Kunisawa, J. Thorner, A putative protein kinase overcomes pheromone-induced arrest of cell cycling in S. cerevisiae. *Cell* **58**, 1107–1119 (1989).

27. H. D. Madhani, C. A. Styles, G. R. Fink, MAP Kinases with Distinct Inhibitory Functions Impart Signaling Specificity during Yeast Differentiation. *Cell* **91**, 673–684 (1997).

28. H. D. Madhani, T. Galitski, E. S. Lander, G. R. Fink, Effectors of a developmental mitogen-activated protein kinase cascade revealed by expression signatures of signaling mutants. *Proc. Natl. Acad. Sci. U.S.A.* **96**, 12530–12535 (1999).

29. J. Barrere, P. Nanda, A. W. Murray, Alternating selection for dispersal and multicellularity favors regulated life cycles. *Current Biology* **33**, 1809-1817.e3 (2023).

30. E. A. Musgrove, C. E. Caldon, J. Barraclough, A. Stone, R. L. Sutherland, Cyclin D as a therapeutic target in cancer. *Nat Rev Cancer* **11**, 558–572 (2011).

31. E. S. Knudsen, K. E. Knudsen, Tailoring to RB: tumour suppressor status and therapeutic response. *Nat Rev Cancer* **8**, 714–724 (2008).

32. A. M. Nedelcu, The evolution of multicellularity and cancer: views and paradigms. *Biochemical Society Transactions* **48**, 1505–1518 (2020).

33. T. Pradeu, *et al.*, Reuniting philosophy and science to advance cancer research. *Biological Reviews* brv.12971 (2023). https://doi.org/10.1111/brv.12971.

34. F. Sherman, "[1] Getting started with yeast" in *Methods in Enzymology*, (Elsevier, 1991), pp. 3–21.

35. D. Gietz, A. St. Jean, R. A. Woods, R. H. Schiestl, Improved method for high efficiency transformation of intact yeast cells. *Nucl Acids Res* **20**, 1425–1425 (1992).

FIGURES LEGENDS

Figure 1. Competition experiments.

A. Experimental set-up of the co-culture competition experiments between *ace2/ace2* and *ACE2/ACE2* strains. A 50/50 mix of the two strains based either on phenotype (snowflake vs planktonic) or on genotype (*ace2* vs *ACE2*) was inoculated in SDcasaWAU liquid medium. The resulting co-culture was grown for 2 days until a stationary phase was reached and then diluted again in fresh medium. At each dilution step, the proportion of the snowflake phenotype or *ace2* genotype was determined (by microscopy or qPCR respectively). **B.** Evolution of the percentage of snowflake entities during independent co-culture competitions between *ace2/ace2* and *ACE2/ACE2* strains, either *cln3/cln3* (red bars) or *CLN3/CLN3* (black bars) (N=4, n>250, mean ± SD, ns p>0.05, *p<0.05, ***p<0.001). The percentage of snowflakes is statistically compared between *CLN3/CLN3* and *cln3/cln3* co-cultures at each dilution round, using a Fisher's exact test. **C.** The proportion of *ace2/ace2* genotype was monitored by qPCR in independent competitions in cln3/cln3 (red bars) and CLN3/CLN3 (black bars) backgrounds. The *ACT1* locus, amplified in all the cells of the population, was used to normalize the proportion of *ace2* cells in the co-culture cell population (N=3, mean ± SD, unpaired t-test, Welch correction, ns p>0.05, ***p<0.001). **D.** Evolution of the percentage of snowflake entities during independent co-culture competitions between *ace2/ace2* and *ACE2/ACE2* strains overexpressing *WHI5* (orange bars) or not (black bars) (N=3, n>235, mean ± SD, Fisher's exact test, ns p>0.05, *p<0.05, **p<0.005, ***p<0.001).

Figure 2. Stationary phase exit efficiency explains the results of competition experiments.

A. Quantification of the lag duration upon refeeding in fresh SDCasaWAU liquid medium after 2 days of growth. The optical density at 600nm was followed upon refeending for each independent culture (N=4, mean ± SD, unpaired t-test, Welch correction, ns p>0.05, ***p<0.001). **B.** Representative image series of *cln3/cln3* cells either *ace2/ace2* or *ACE2/ACE2* upon refeeding of 2-day cultures on a fresh SDCasaWAU medium microscope pad. Arrows point to bud emergence. Bars are 10µm. **C.** Proportion of *cln3/cln3* cells that have formed a new bud upon refeeding on a fresh SDCasaWAU medium microscope pad of either *ace2/ace2* or *ACE2/ACE2* 2-day cultures (N=3, n>101, Fisher's exact test, mean ± SD, ns p>0.05, *p<0.05, **p<0.005, ***p<0.001). **D.** Same as C in a *cln3* haploid background (N=3, n>100, mean ± SD, Fisher's exact test, **p<0.005, ***p<0.001). **E.** Percentage of snowflake entities observed in independent co-cultures of *ace2/ace2* and *ACE2/ACE2* strains. Cultures either went through cycles of proliferation and stationary phase as described in Fig1A (right panel), or maintained in constant exponential phase (left panel) (N>3, n>208, mean ± SD, Fisher's exact test, ns

p>0.05). **F.** Same as A except that the refeeding was done after a culture of 5 days (N=3, mean ± SD, unpaired t-test, Welch correction, **p<0.005). **G.** Percentage of snowflake entities observed in independent co-cultures of *ace2/ace2* and *ACE2/ACE2* strains diluted every two days (red and black bars) or every five days (grey and pink bars) (N≥3, n>700, mean ± SD, Fisher's exact test, ns p>0.05, **p<0.005, ***p<0.001).

Figure 3. Snowflake characterization and stationary phase exit efficiency of quintuple mutant strains.

A. Representative image of the quintuple mutant strain. Bar is 10µm. **B.** Size distribution of quintuple mutant (triangles) or *ace2/ace2* (circles) snowflakes. Size is estimated by measuring both the longest segment of the snowflake entity and the longest segment perpendicular to the first one. We compared the length of each segment independently with an unpaired t-test with a Welch correction (N=3, n>60, mean ± SD). **C.** Proportion of snowflake entities in a population of quintuple mutant or *ace2/ace2* strains (N=3, n>201, mean ± SD, Fisher's exact test, ns p>0.05). **D.** Proportion of *cln3/cln3* cells, either quintuple mutant or WT, that formed a new bud upon refeeding of 2-days cultures on a fresh SDCasaWAU medium microscope pad (N=3, n>102, mean ± SD, Fisher's exact test, ns p>0.05, *p<0.05). **E.** Proportion of *cln3/cln3* cells, either quintuple mutant or *ace2/ace2*, that formed a new bud upon refeeding of 2-days cultures on a fresh SDCasaWAU medium microscope pad (N=3, n>75, mean ± SD, Fisher's exact test, ns p>0.05, *p<0.05, **p<0.005, ***p<0.001). **F.** Evolution of the percentage of snowflake entities during independent co-culture competitions between quintuple mutant and WT strains either *cln3/cln3* (red bars) or *CLN3/CLN3* (black bars) (N=3, n>250, mean ± SD, Fisher's exact test).

Figure 4. Faster exit from stationary phase of ace2 cln3 cells depends on the ace2 mutation and not on the Snowflake phenotype.

A. A 2-days *ace2/ace2 cln3/cln3* culture was sonicated and refed onto a fresh SDCasaWAU microscope pad. The proportion of cells that formed a new bud upon refeeding was assessed within different multicellular size ranges (N=3, n>184, mean ± SD, Fisher's exact test). **B.** 2 days *cln3* cultures, either *ace2* or *ACE2*, were sonicated and refed onto a fresh SDCasaWAU microscope pad. Within entities formed of 1 to 3 cells, the proportion of cells that formed a new bud upon refeeding was assessed (N=3, n>63, mean ± SD, Fisher's exact test, ns p>0.05, *p<0.05, **p<0.005, ***p<0.001).

Figure 5. Faster exit from stationary phase of *ace2 cln3* cells is dependent on the Kss1 MAP kinase, which favors transcription of the *CLN1* cyclin gene.

A. Proportion of *cln3 kss1* cells, either ace2 or ACE2, that formed a new bud upon refeeding of 2-day cultures on a fresh SDCasaWAU medium microscope pad (N=3, n>86, mean ± SD, Fisher's exact test, ns p>0.05). **B**. Ratio of *CLN1* mRNA level and *ACT1* mRNA level, determined by RT-qPCR, 15 minutes upon refeeding of 2 days *cln3* cultures, either *ace2* or *ACE2* (N=3, mean ± SD, unpaired t-test, Welch correction, **p<0.005). **C**. Ratio of *CLN1* mRNA level and *ACT1* mRNA level, determined by RT-qPCR, 15 minutes upon refeeding of 2 days *kss1 cln3* cultures, either *ace2* or *ACE2* (N=3, mean ± SD, unpaired t-test, Welch correction, ns p>0.05).

Figure 6. Snowflake characterization, stationary phase exit efficiency and selection in competition experiments of Snowflake AMN1-368D strains.

A. Representative image of the *AMN1-368D* strain. Bar is 10µm. **B.** Proportion of snowflake entities in populations of *AMN1-368D* or *ace2* haploid strains (N=3, n>219, mean ± SD, Fisher's exact test, ns p>0.05). **C.** Size distribution of *AMN1-368D* (diamond) or *ace2* (circle) snowflakes. Size is estimated by measuring both the longest segment of the snowflake entity and the longest segment perpendicular to the first one (N=3, n>74, mean ± SD, unpaired t-test, Welch correction, ***p<0.001, account for both segment). **D.** Proportion of *cln3* cells, either *AMN1-368D* or *AMN1-368V*, that formed a new bud upon refeeding of 2-day cultures on a fresh SDCasaWAU medium microscope pad (N=3, n>77, mean ± SD, Fisher's exact test, ns p>0.05, *p<0.05, **p<0.005, ***p<0.001). **E.** Evolution of the percentage of snowflake entities during independent co-culture competitions between *AMN1-368D* and *AMN1-368V* strains, either *cln3/cln3* (red bars) or *CLN3/CLN3* (black bars) (N=3, n>252, mean ± SD, Fisher's exact test, ns p>0.05, **p<0.005, ***p<0.001). **F.** Evolution of the percentage of snowflake entities during independent co-culture competitions between *AMN1-368D* and *AMN1-368V* strains overexpressing *WHI5* (orange bars) or not (black bars) (N=3, n>302, Fisher's exact test, ns p>0.05, **p<0.005, ***p<0.001).

Figure 7. Model explaining the selection of the Snowflake phenotype as a passenger phenotype.

In lab strains (**A**), a default in stationary phase exit upon refeeding was observed in a *cln3* mutant. In feral strains (**B**), the functional *AMN1-368D* allele leads to degradation of Ace2p, which can no longer repress the expression of the Kss1 Map kinase. Kss1p favors the transcription of *CLN1*, which would favor progression to S phase and partially suppress the default in stationary phase associated with the

cln3 mutation. This observed selective advantage (a) leads to the selection of *AMN1-368D* genotype (b), and because of the pleiotropy of Ace2p transcription factor, to the selection of the Snowflake multicellular phenotype as a passenger phenotype (c).

Figure 1

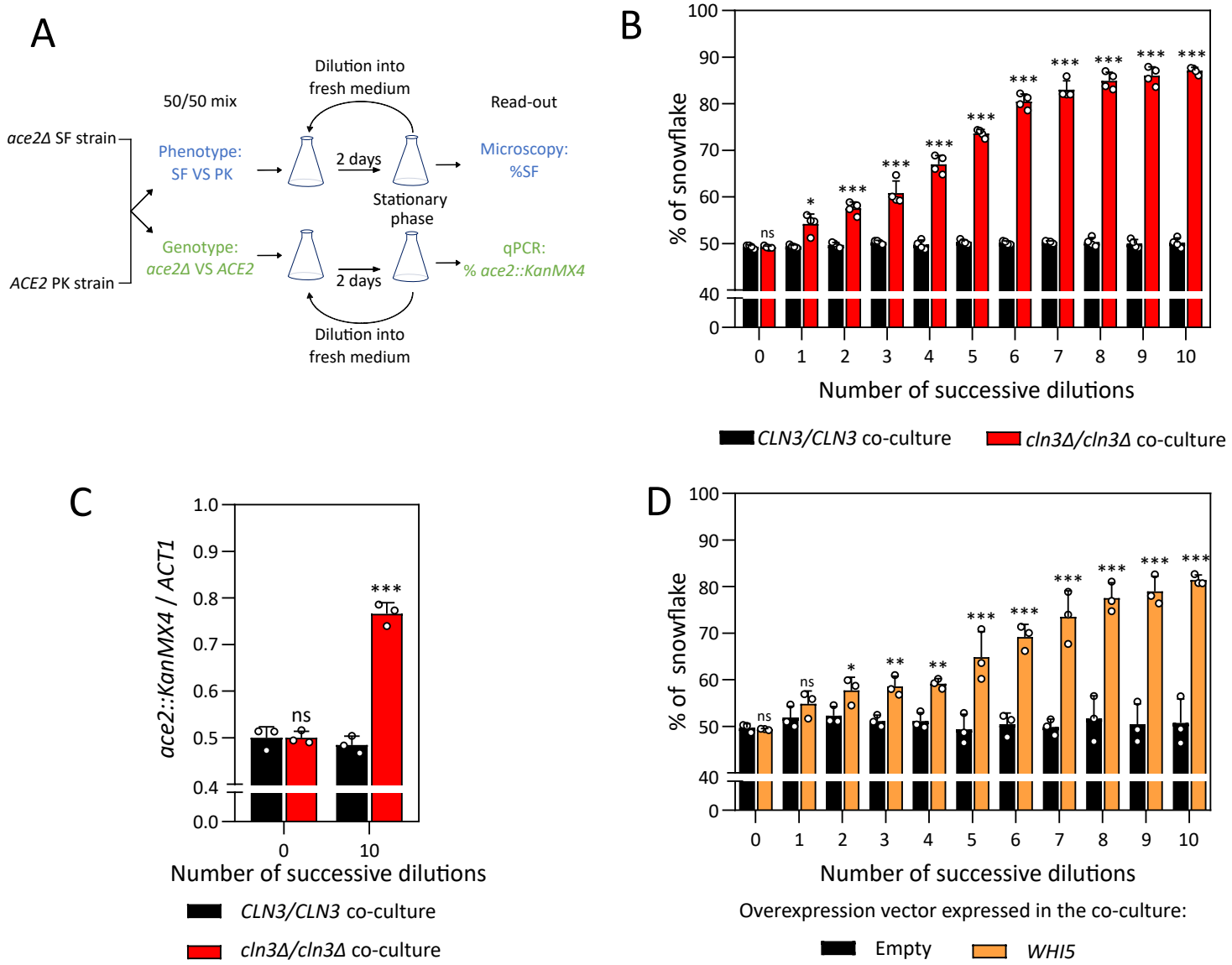
A
50/50 mix
ace2Δ SF strain
ACE2 PK strain
Phenotype:
SF VS PK
Genotype:
ace2Δ VS ACE2
Dilution into
fresh medium
2 days
Stationary
phase
2 days
Dilution into
fresh medium
Read-out
Microscopy:
%SF
qPCR:
% ace2::KanMX4
B
% of snowflake
Number of successive dilutions
CLN3/CLN3 co-culture
cln3Δ/cln3Δ co-culture
C
ace2::KanMX4 / ACT1
Number of successive dilutions
CLN3/CLN3 co-culture
cln3Δ/cln3Δ co-culture
D
% of snowflake
Number of successive dilutions
Overexpression vector expressed in the co-culture:
Empty
WHI5

Figure 2

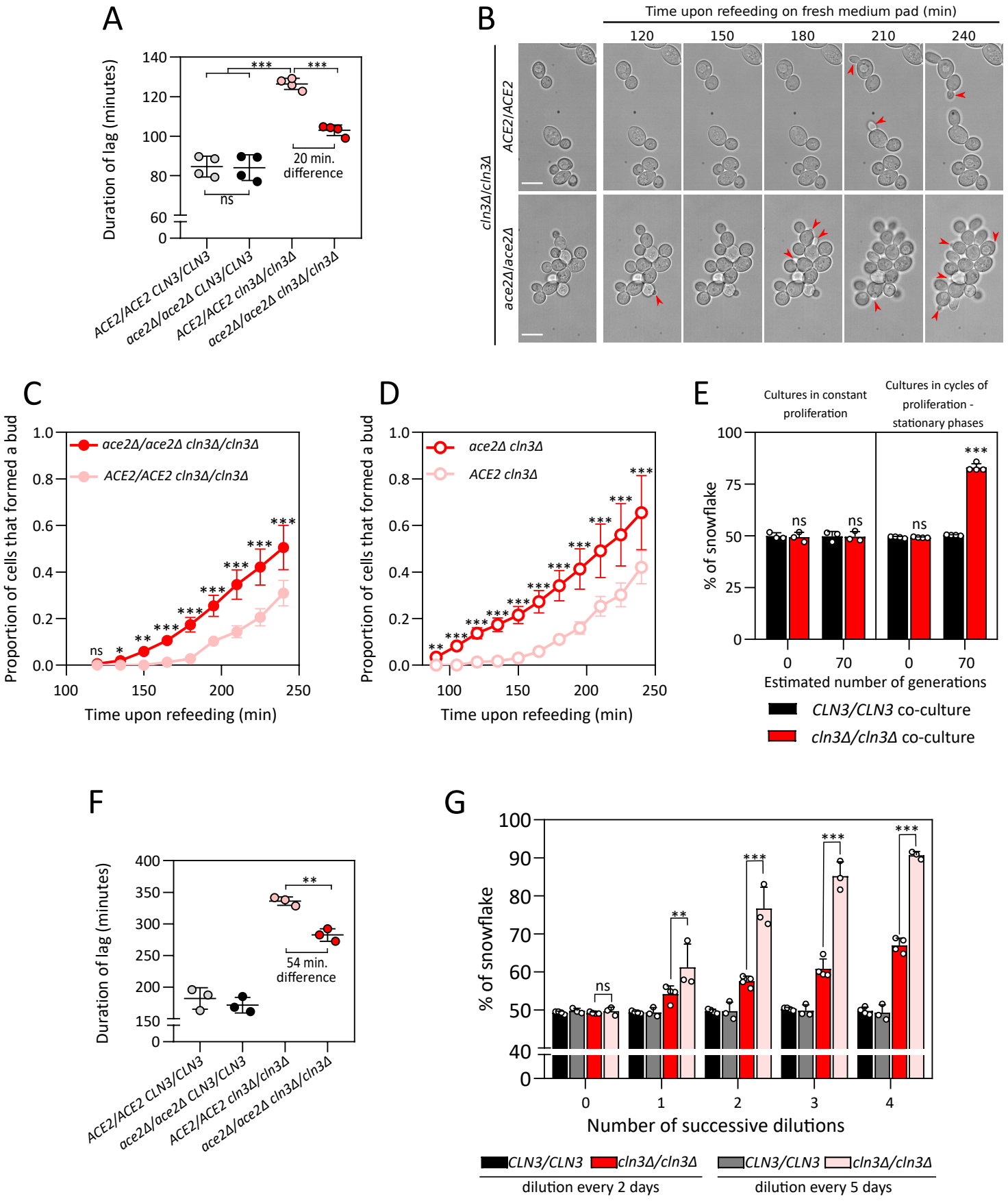
A
Duration of lag (minutes)
140
120
100
80
60
0
***
***
ns
20 min.
difference
ACE2/ACE2 CLN3/CLN3
ace2Δ/ace2Δ CLN3/CLN3
ACE2/ACE2 cln3Δ/cln3Δ
ace2Δ/ace2Δ cln3Δ/cln3Δ
B
Time upon refeeding on fresh medium pad (min)
120
150
180
210
240
ACE2/ACE2
cln3Δ/cln3Δ
ace2Δ/ace2Δ
C
Proportion of cells that formed a bud
ace2Δ/ace2Δ cln3Δ/cln3Δ
ACE2/ACE2 cln3Δ/cln3Δ
Time upon refeeding (min)
D
Proportion of cells that formed a bud
ace2Δ cln3Δ
ACE2 cln3Δ
Time upon refeeding (min)
E
Cultures in constant proliferation
Cultures in cycles of proliferation - stationary phases
% of snowflake
Estimated number of generations
CLN3/CLN3 co-culture
cln3Δ/cln3Δ co-culture
F
Duration of lag (minutes)
54 min.
difference
ACE2/ACE2 CLN3/CLN3
ace2Δ/ace2Δ CLN3/CLN3
ACE2/ACE2 cln3Δ/cln3Δ
ace2Δ/ace2Δ cln3Δ/cln3Δ
G
% of snowflake
Number of successive dilutions
CLN3/CLN3
cln3Δ/cln3Δ
CLN3/CLN3
cln3Δ/cln3Δ
dilution every 2 days
dilution every 5 days

Figure 3

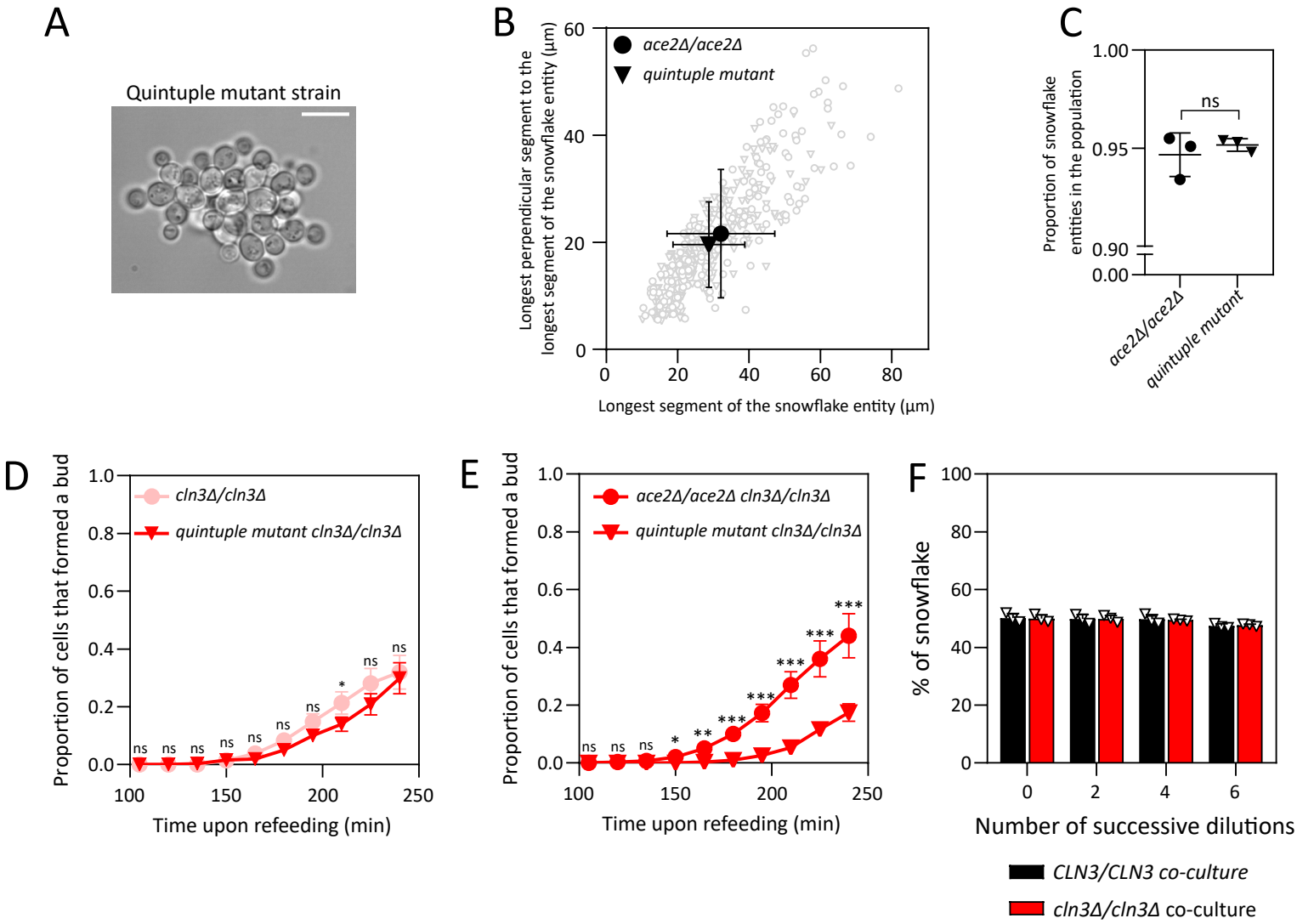
A
Quintuple mutant strain
B
ace2Δ/ace2Δ
quintuple mutant
Longest perpendicular segment to the longest segment of the snowflake entity (µm)
Longest segment of the snowflake entity (µm)
C
Proportion of snowflake entities in the population
ns
ace2Δ/ace2Δ
quintuple mutant
D
cln3Δ/cln3Δ
quintuple mutant cln3Δ/cln3Δ
Proportion of cells that formed a bud
Time upon refeeding (min)
E
ace2Δ/ace2Δ cln3Δ/cln3Δ
quintuple mutant cln3Δ/cln3Δ
Proportion of cells that formed a bud
Time upon refeeding (min)
F
% of snowflake
Number of successive dilutions
CLN3/CLN3 co-culture
cln3Δ/cln3Δ co-culture

Figure 4

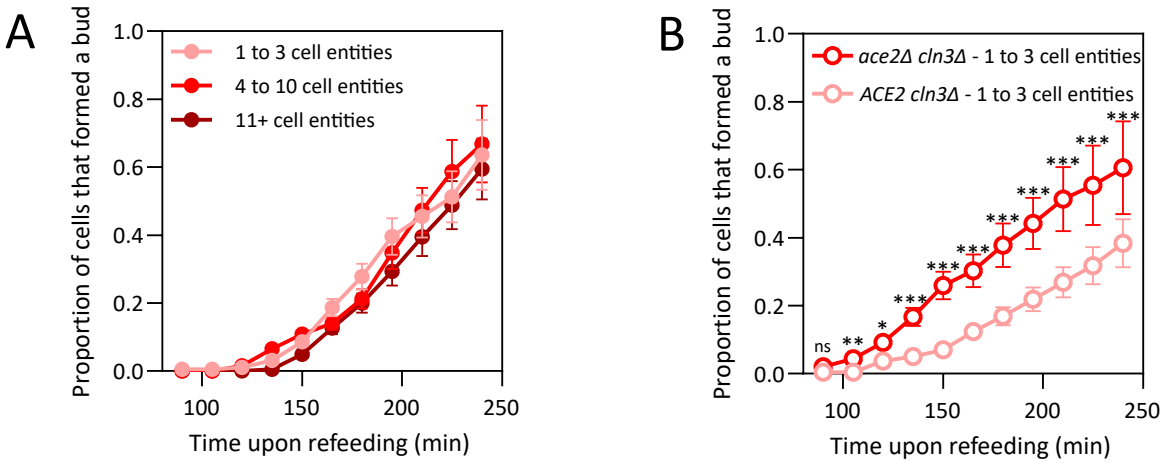
A
Proportion of cells that formed a bud
1.0
0.8
0.6
0.4
0.2
0.0
1 to 3 cell entities
4 to 10 cell entities
11+ cell entities
100
150
200
250
Time upon refeeding (min)
B
Proportion of cells that formed a bud
1.0
0.8
0.6
0.4
0.2
0.0
ace2Δ cln3Δ - 1 to 3 cell entities
ACE2 cln3Δ - 1 to 3 cell entities
ns
**
*
***
100
150
200
250
Time upon refeeding (min)

Figure 5

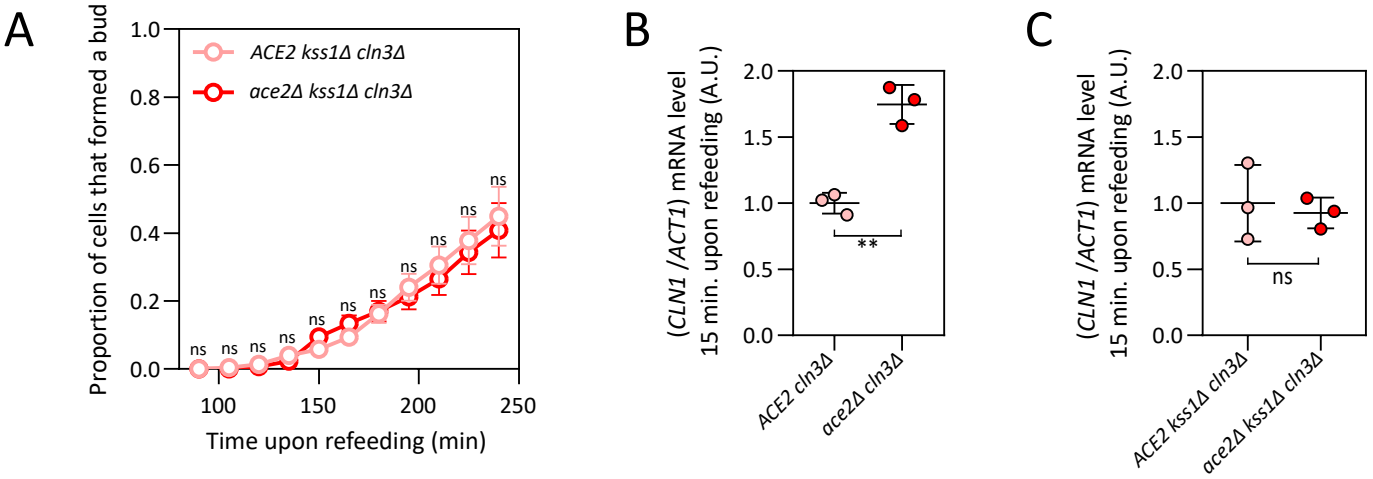
A
Proportion of cells that formed a bud
1.0
0.8
0.6
0.4
0.2
0.0
ACE2 kss1Δ cln3Δ
ace2Δ kss1Δ cln3Δ
ns
100
150
200
250
Time upon refeeding (min)
B
(CLN1 /ACT1) mRNA level
15 min. upon refeeding (A.U.)
2.0
1.5
1.0
0.5
0.0
**
ACE2 cln3Δ
ace2Δ cln3Δ
C
(CLN1 /ACT1) mRNA level
15 min. upon refeeding (A.U.)
ns
ACE2 kss1Δ cln3Δ
ace2Δ kss1Δ cln3Δ

Figure 6

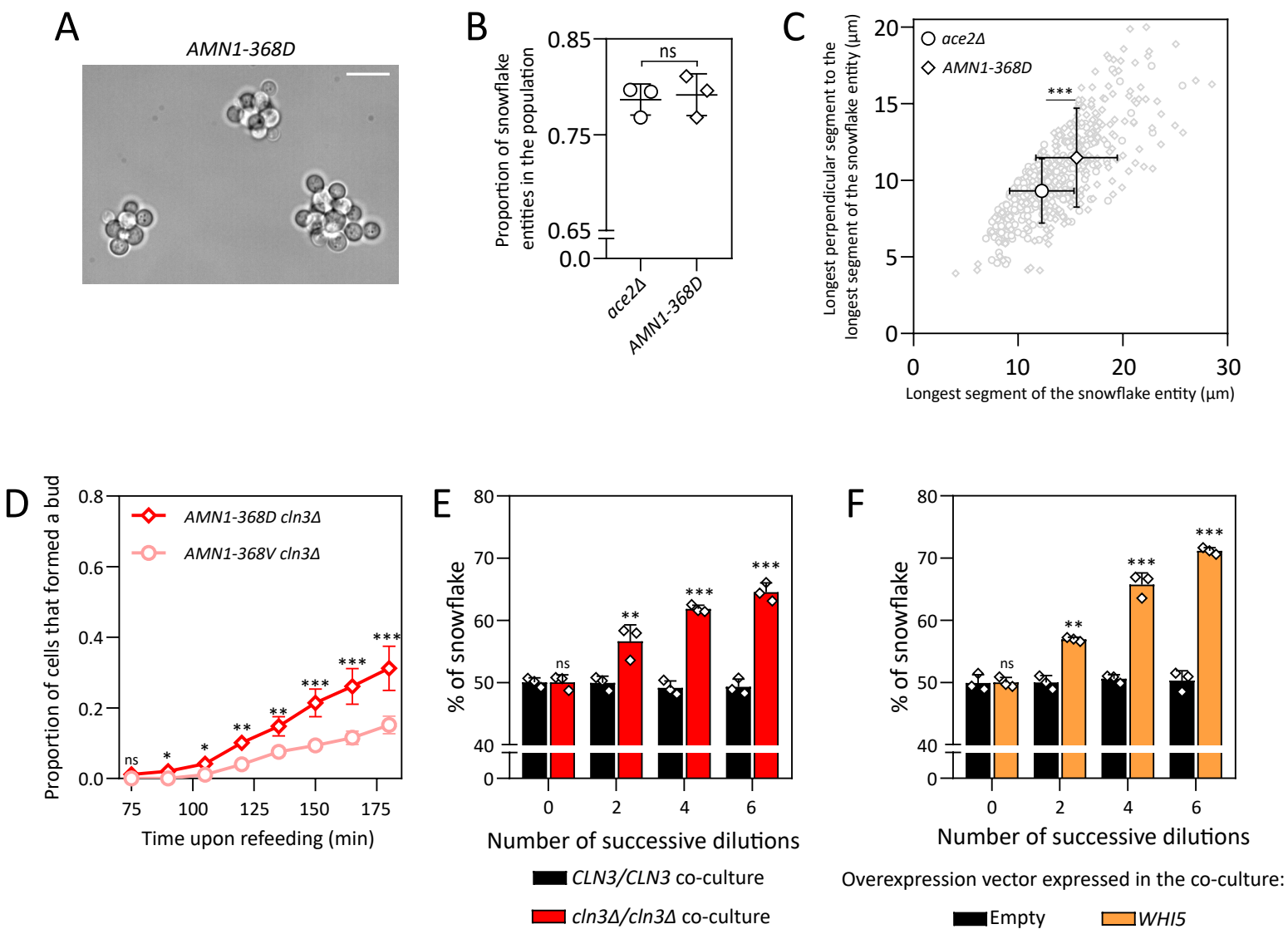
A
AMN1-368D
B
Proportion of snowflake entities in the population
0.85
0.75
0.65
0.0
ns
ace2Δ
AMN1-368D
C
Longest perpendicular segment to the longest segment of the snowflake entity (µm)
ace2Δ
AMN1-368D
***
Longest segment of the snowflake entity (µm)
D
Proportion of cells that formed a bud
AMN1-368D cln3Δ
AMN1-368V cln3Δ
Time upon refeeding (min)
E
% of snowflake
Number of successive dilutions
CLN3/CLN3 co-culture
cln3Δ/cln3Δ co-culture
F
% of snowflake
Number of successive dilutions
Overexpression vector expressed in the co-culture:
Empty
WHI5

Figure 7

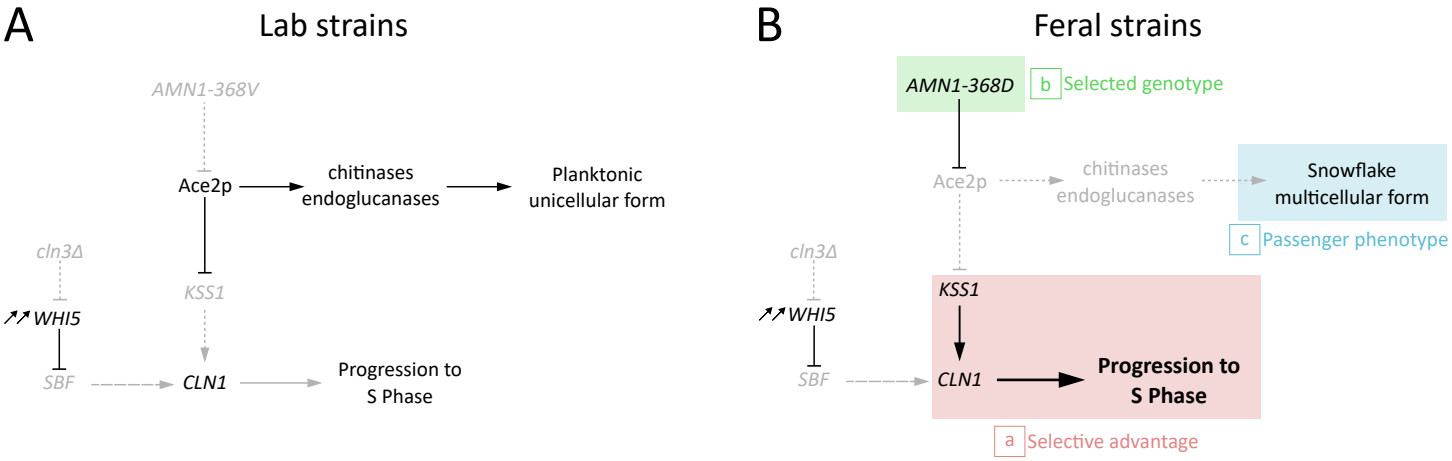
A
Lab strains
AMN1-368V
Ace2p
chitinases
endoglucanases
Planktonic
unicellular form
cln3Δ
KSS1
WHI5
SBF
CLN1
Progression to
S Phase
B
Feral strains
AMN1-368D
b Selected genotype
Ace2p
chitinases
endoglucanases
Snowflake
multicellular form
c Passenger phenotype
cln3Δ
KSS1
WHI5
SBF
CLN1
Progression to
S Phase
a Selective advantage